Developmental Biology 526 (2025) 70–81

Contents lists available at ScienceDirect

Developmental Biology

journal homepage: www.elsevier.com/locate/developmentalbiology

Original research article

Divergent *Hox* cluster collinearity in horned beetles reveals adult head patterning function of *labial*

Erica M. Nadolski *, Isabel G. Manley, Sukhmani Gill, Armin P. Moczek

Department of Biology, Indiana University, Bloomington, IN, USA

ARTICLE INFO

Keywords:
Intercalary segment
Proboscipedia
Deformed
Homeosis
Beetle horns

ABSTRACT

Hox genes play critical roles in specifying the regionalization of the body axis across metazoa, with the exception of the anterior dorsal head of bilaterian animals, which instead is instructed by a deeply conserved set of non-*Hox* regulators. The anterior dorsal head is also a hot spot of evolutionary diversification, raising the question as to the developmental-genetic underpinnings of such innovation. Onthophagine dung beetles develop evolutionarily novel and highly diversified horns on the dorsal head used as weapons during intrasexual conflicts. Preliminary RNAseq data unexpectedly documented *Hox* gene expression in the dorsal head of premetamorphic onthophagine larvae. Motivated by this observation, we aimed to (i) investigate the genomic content and arrangement of the *Hox* cluster across three onthophagine species, and (ii) assess expression patterns and (iii) potential functions of the anterior Hox genes *labial, proboscipedia*, and *Deformed* in patterning the adult beetle head and cephalic horns. We document an unexpected derived *Hox* cluster configuration in the *Onthophagus sagittarius* genome, a species with apomorphic cephalic horn morphology. Yet despite this genomic rearrangement, embryonic expression patterns of *labial* and *proboscipedia* as well as the adult segment patterning functions of *proboscipedia* and *Deformed* were found to be conserved. In contrast, *labial* RNAi revealed an adult head patterning function outside horn-forming regions previously undescribed for any insect. Lastly, we show that electrosurgical ablation of the presumptive larval *labial*-expressing head region phenocopies this conspicuous adult *labial* RNAi defect. We discuss the implications of these data for current models of insect head development and diversification.

1. Introduction

The majority of the arthropod body is composed of serially homologous segments that differentiate as instructed by *Hox* gene expression along the anteroposterior axis during early embryonic development (Lewis, 1978; Carroll, 1995). A major exception to this rule is the anterior-most region of the embryo, the ocular/protocerebral region (for simplicity, ocular region), which is patterned by a set of non-*Hox* regulators and is considered to be non-segmental in origin (Rogers and Kaufman, 1997; Abzhanov and Kaufman, 1999; Posnien et al., 2011; Zattara et al., 2016). Those segments that are patterned by Hox genes undergo homeotic (identity) transformations when the corresponding *Hox* genes are functionally manipulated (Hughes and Kaufman, 2002; Brown et al., 2002). These data were historically interpreted to mean that the post-embryonic head is made up of segments consisting of both ventral and dorsal components, matching the basic architecture of their thoracic and abdominal counterparts (Snodgrass, 1935, Fig. 1A, top). However, studies in a variety of insect orders have documented that dorsal head structures remain unaffected after *Hox* manipulations (Rogers et al., 2002; Posnien and Bucher, 2010; Smith and Jockusch, 2014). A later hypothesis termed the *bend-and-zipper* model incorporates this observation by positing that the dorsal head instead originates via the upfolding, posterior bending, and fusing of the *Hox*-free and non-segmental antero-lateral embryonic primordia, with gnathal *Hox*--expressing segments contributing only to the ventral head (Posnien and Bucher, 2010; Posnien et al., 2010, Fig. 1A and B). This newer model has successfully incorporated the bulk of existing data on insect head morphogenesis during the transition from the embryonic to juvenile stage but is agnostic to morphogenetic dynamics during the metamorphic transition from the juvenile to adult stage.

In addition to being a presumptively *Hox*-free region, the dorsal head of insects is also a hot spot of evolutionary innovation, having given rise to *e.g.* the weevil rostrum, the stalks of stalk-eyed flies, and the cephalic horns of scarab beetles. Yet, how morphological novelties such as horns and stalks may originate and then integrate within deeply conserved trait complexes such as the dorsal head without compromising ancestral

* Corresponding author.
E-mail address: emnadols@iu.edu (E.M. Nadolski).

https://doi.org/10.1016/j.ydbio.2025.07.002
Received 7 April 2025; Received in revised form 1 July 2025; Accepted 2 July 2025
Available online 3 July 2025

functions remains largely unclear. Horned dung beetles, in particular, are famous for their extraordinarily diversified dorsal cephalic horns, a textbook example of evolutionary novelties (Emlen et al., 2005). In the horned dung beetle genus *Onthophagus* alone, cephalic horns differ in number, positioning, and relative size as a function of species, sex, and sometimes simply adult size. Ancestral state reconstructions suggest, however, that this enormous diversity was initiated when male *Onthophagus* evolved the ability to form one or multiple horns in the posterior head specifically (Emlen et al., 2005). Ablation-based fate mapping studies in two species exhibiting this ancestral pattern of horn growth – *Onthophagus taurus* and *Digitonthophagus gazella* – determined that paired posterior head horns are positioned roughly along the boundary between the clypeolabral and ocular regions, both of which form from within the non-segmental anterior-most embryonic head (Busey et al., 2016). A closely related species, *O. sagittarius*, exhibits a derived horn morphology in the dorsal posterior head, with males *repressing* posterior horn formation (Kijimoto et al., 2012) and females sporting a single, medial head horn. Fate mapping of the female horn indicated a different regional origin, arising instead from fully within the boundaries of the clypeolabral region (Busey et al., 2016).

A subset of onthophagine species also possess independently evolved *prothoracic horns*, which recent studies have identified as partial serial homologs of the meso- and metathoracic wings of insects, as well as other dorsal and dorsolateral traits including the bilateral gin traps observed in the abdomen of *Tribolium* and *Tenebrio* pupae (Hu and Moczek, 2021; Ohde et al., 2013). One key piece of evidence in support of this conclusion derived from the observation that RNAi-mediated transcript depletion of *Sex combs reduced*, the *Hox* gene instructing prothorax identity, contributes to the transformation of the prothoracic horn of *Onthophagus* beetles into ectopic wings, a key requirement for establishing (serial) homology (Hu et al., 2019). In contrast, the evolutionary origins of head horns remain largely unclear, including the possibility of anterior *Hox* gene involvement. However, recent work utilizing head-region-specific RNAseq raised precisely this possibility. Specifically, a comparative transcriptomic study in *O. taurus* wherein lateral, medial, posterior, and anterior regions of the dorsal head epithelium were microdissected and sequenced as separate libraries found the two anterior-most *Hox* genes *labial* and *proboscipedia* to be upregulated in posterolateral head regions (Linz and Moczek, 2020, Fig. 1C). These data stand at odds with predictions made by the *bend--and-zipper* model as well as general understanding of insect head evolution which instead assumes *Hox* patterning to be restricted to ventral portions of the head (Fig. 1A).

Motivated by the documentation of *Hox* gene expression in the dorsal head of horned beetle larvae, we aimed to first investigate the genomic arrangement of the *Hox* cluster in three onthophagine species. We then assessed the expression patterns of the anterior *Hox* genes *labial* and *proboscipedia* using *in situ* Hybridization Chain Reaction (HCR), followed by a combination of larval RNAinterference (RNAi) and electrosurgical ablation approaches to investigate their possible function in patterning the adult beetle head and/or cephalic horns. More generally, we aimed to use these data to further our understanding of the segmental contributions to the adult beetle head and to reconcile the *bend-and-zipper* model of insect head development with the dorsal *Hox* expression data observed in horned dung beetles.

2. Methods

2.1. Assessing genomic content and arrangement of Hox clusters

Custom BLAST databases were generated for the *O. sagittarius*, *O. taurus,* and *D. gazella* proteomes (Davidson and Moczek, 2024) using

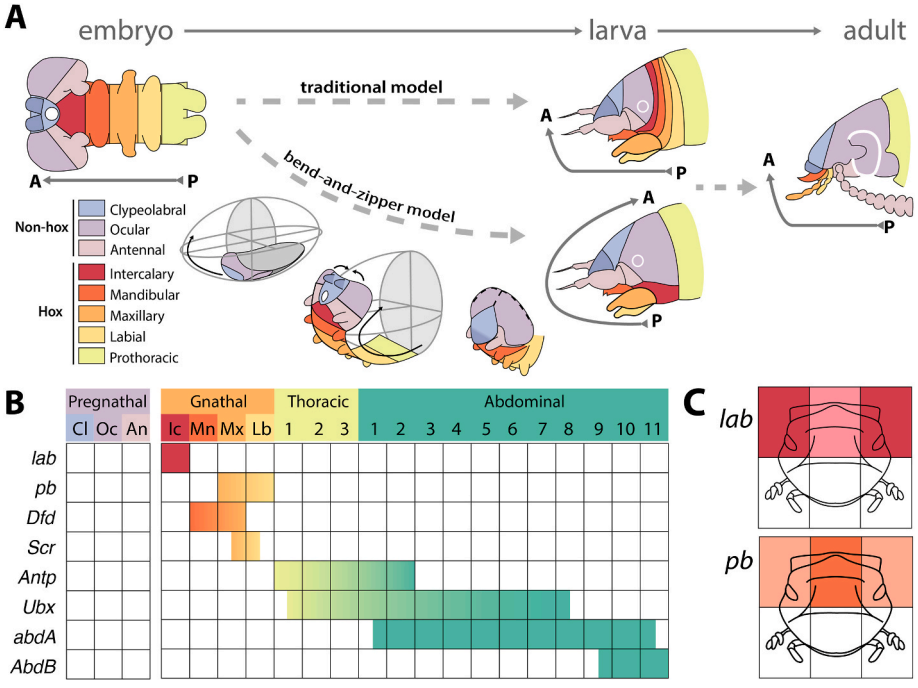

Fig. 1. Current models of insect head morphogenesis and *Hox* gene expression data across beetles. To contrast the traditional model of insect head development, Posnien et al. (2010) proposed the bend-and-zipper model, wherein the anterior end of the flat early embryo folds upward and then fuses along the dorsal midline to meet the prothoracic segment (A). This model accounts for *Tribolium* data documenting that parental RNAi of *Hox* genes affects only ventral, mouthpart-bearing regions or the lateral gena but leaves the dorsal head of larvae unaffected. Additional work in *Tribolium* recapitulated these mouthpart transformations in adults after larval *Hox* RNAi (A, right). Expression patterns of each *Hox* gene along the segmented *Tribolium* embryo are shown in (B, colored boxes). Transcriptomic data from sections of the dorsal head epithelium of pre-pupal *O. taurus* document expression of *lab* and *pb* in the posterior half of the dorsal head, color coded by expression level (C). Segment abbreviations: Cl – clypeolabral; Oc – ocular; An – Antennal; Ic – Intercalary; Mn– mandibular; Mx – maxillary; Lb – labial; [Diagrams in A are based on Posnien et al., 2010 (Figs. 1C and 2B-D), Posnien and Bucher 2010; Smith and Jockusch 2014; data in B from Brown et al., 2002, data in C from Linz and Moczek 2020]. (For interpretation of the references to color in this figure legend, the reader is referred to the Web version of this article.)

command-line BLAST+ (Altschul et al., 1990). *Drosophila melanogaster Hox* gene protein sequences were downloaded from Flybase (version FB2024_02, Öztürk-Çolak et al., 2024) as queries. The query sequences were used to search the beetle proteome databases to identify target protein sequences for the eight canonical insect Hox genes involved in regionalization of the anteroposterior body axis: *Labial, Proboscipedia, Deformed, Sex combs reduced, Antennapedia, Ultrabithorax, Abdominal-A* and *Abdominal-B*. We established an e-value cutoff of 1×10^{-5} for selecting the best hit from each list of potential targets and manually validated the top hits with the end-to-end sequence alignment tool MUSCLE (MUltiple Sequence Comparison by Log-Expectation, Madeira et al., 2024). The genomic start and end coordinates of each *Hox* gene were then mapped onto chromosome-level genome assemblies for each species (Davidson and Moczek, 2024) to assess cluster arrangement (Supplementary Table 1). Upon discovering an unexpected arrangement of the cluster in one genome, we wanted to secondarily validate this finding; to do so, we reconstructed the contigs generated during genome sequencing from the raw PacBio HiFi CCS long-read sequencing data via *hifiasm v. 0.13* under default parameters (Cheng et al., 2021), which we then examined for the presence of the entire derived *Hox* cluster configuration on a single contiguous segment of sequenced genomic DNA (Supplementary Table 2). The program MCScanX was used to detect colinear blocks of genes on the chromosomes containing the *Hox* cluster in the three genomes (Wang et al., 2024). Synteny of these contiguous blocks was visualized using SynVisio to map *Hox* gene arrangement and overall genomic architecture along the chromosomes (Bandi and Gutwin, 2020).

2.2. Beetle husbandry

Onthophagus sagittarius individuals were collected near Kilcoy, Queensland, AU (−26.951, 152.605), and *O. taurus* individuals were collected near Chapel Hill, North Carolina, USA (35.936, −79.128). Both species were reared in lab colonies as described previously (Moczek and Nagy, 2005). Reproductively active adults were transferred from the colonies into breeding containers and allowed to reproduce. After one week, eggs and eclosed larvae were transferred from their natal brood balls into twelve-well plates provisioned with cow dung from Marble Hill Farm, Bloomington, Indiana, USA, as described in Shafiei et al. (2001). Plates with larvae were kept at a 16:8h light/dark cycle throughout development, with *O. taurus* incubated at 24 °C and *O. sagittarius* incubated at 28 °C pre- and post-injection until eclosion. Eclosed experimental adults were sacrificed and preserved in 70 % ethanol.

2.3. Embryonic dissections and in situ hybridization chain reaction

We selected *O. sagittarius* embryos within three days of egg-laying for sample preparation. The embryos were dissected out of their eggshells in 8 % formaldehyde (FA) solution and allowed to fix for 40 min at room temperature. After several washes with 0.1 % Tween-20 in phosphate-buffered saline (PBST), the tissue was dehydrated through a methanol wash series. The samples were stored in 100 % methanol overnight at −20 °C, rehydrated through a wash series of methanol in PBST, and rinsed several times in PBST. Tissues were then subjected to a 5-min proteinase K (10 μg/μl) digestion, rinsed several times in PBST, post-fixed in 3.7 % FA for 20 min, and washed in PBT. The samples were subsequently processed using standard procedures of third generation *in situ* hybridization chain reaction (*in situ* HCR v3.0) (Choi et al., 2018). DAPI counterstain was also applied to the tissues to visualize nuclei. After several washes in sodium chloride sodium citrate buffer with 0.05 % Triton-X, tissues were mounted on a glass slide in glycerol. HCR probes for the *Hox* genes were designed to avoid the homeobox region to circumvent non-specific binding. Probe sequences were designed by Molecular Instruments. A Leica Stellaris 8 confocal microscope equipped with a HC PL APO CS2 10x/0.40 dry objective was used to image whole-mount embryos using a white light laser (WLL: 440 nm–790 nm) and a Diode 405 nm laser, acousto-optical tunable filter, a pinhole of 1 AU, and the following detectors per fluorophore (target, fluorophore, detector, emission tuning/gain/offset): DAPI, HyD S1, 420–510nm/91/0; *Os-pb*, AlexaFluor488, HyD S1, 505–560nm/53/0; *Os-lab*, AlexaFluor647, HyD X3 660–780nm/98/0. In situ HCR staining was also attempted on whole-mount pre-metamorphic head tissue, but due to the early timing of cuticle deposition by the head epithelium during the larval-to-pupal molt, cuticle autofluorescence presented a challenge to visualization that we were not able to overcome to assess clear expression patterns at this timepoint.

2.4. Double-stranded RNA synthesis and injection for RNA interference

Fragments of each target gene for RNA interference (RNAi) were chosen by using a BLAST algorithm to query 250bp regions of each gene against the *O. taurus* or *O. sagittarius* transcriptome and selecting regions with zero off-target hits. One RNAi target region was chosen per gene (Supplementary Table 3). Oligonucleotide constructs for each target and construct-specific primers were designed using the appropriate reference genome (Davidson and Moczek, 2024) and ordered from Integrated DNA Technologies, Inc. Synthesis of double-stranded RNA (dsRNA) for gene knockdown via RNAi was performed using a protocol optimized for coleopteran larvae (Philip and Tomoyasu, 2011). Briefly, for each gene, PCR was performed to anneal T7 RNA polymerase binding sequences to the ends of the gene fragment construct, generating the DNA template for dsRNA synthesis. The Qiagen QIAquick PCR Purification kit was used to purify these constructs. In vitro transcription to generate dsRNA from the DNA template was performed using an Ambion MEGAscript T7 kit, and each product was then purified using an Ambion MEGAclear kit with an ethanol precipitation step (Philip and Tomoyasu, 2011).

Double-stranded RNA constructs for each target gene were diluted to 1 μg/μL with injection buffer (Philip and Tomoyasu, 2011). A Hamilton brand syringe and small gauge removable needle (32 gauge) were used to inject a 3 μl dose of dsRNA targeting a single gene through the abdominal cuticle into the hemolymph of third-instar larvae, to initiate whole-body RNAi (Supplementary Table 4). For experimental treatments targeting multiple genes simultaneously, injection mixture was diluted to a 1 μg/μl concentration per target gene, with injection doses totaling 3ul. Control individuals were randomly selected from each round of developing larvae and injected with pure injection buffer. Previous work in dung beetles has shown that injection of pure buffer alone can serve as a suitable control for dsRNA injection, as neither buffer-injected nor nonsense RNA-injected adults have been documented to show any detectable phenotypic differences compared to wildtype adults (Moczek and Rose, 2009; Simonnet and Moczek, 2011; Linz et al., 2019).

2.5. Fate mapping via electrosurgical ablation of larval head epithelium

A Hyfrecator 2000 electrosurgical unit (ConMed, Utica, NY) was fitted with a metal surgical tip (Epilation/Telangiectasia Needle Stealth ER coating 30 angle, 3/8, 714-S; ConMed) to execute precise ablations of the head epidermis through the head cuticle in both species. Using protocols developed by Busey et al. (2016), we applied 10 Watts for 3 s (*O. taurus*) or 2 s (*O. sagittarius*), respectively, applications found to generate clearly distinguishable phenotypes without causing excess mortality. Three separate posterior dorsal head regions were evaluated, targeting cells on the right side of the head of each treated larvae while leaving the left side of the same head untreated to serve as a negative control. All animals were treated during the last larval instar stage prior to apolysis and epidermal proliferation occurring during the metamorphic transition.

2.6. Phenotype assessment and photography

We analyzed the phenotypes of RNAi-injected, control buffer-injected, and voltage-ablated individuals after eclosion. After sacrificing adult animals, whole heads were dissected away from the body for clarity of viewing. For RNAi and control-injected animals, ventral mouthparts were dissected away from the head for clarity of viewing. Representative individuals from each sample group were photographed using a Leica MZ16 microscope with a PLANAPO 2.0x objective and a Leica S8APO microscope and a PixeLINK PL-D7912CU-T camera; multiple photos of each sample were taken across different planes of focus and overlaid using Adobe Photoshop.

3. Results

Motivated by earlier work documenting unexpected Hox gene expression in the dorsal head of premetamorphic larvae (Linz and Moczek, 2020), we aimed to investigate the genomic Hox cluster across multiple horned dung beetle species, as well as the potential functions of anterior Hox genes *labial, proboscipedia*, and *Deformed* in establishing the segmental boundaries of the adult beetle head and in patterning the cephalic horns contained therein. We first investigated the genomic arrangement and content of the Hox cluster in three species: *D. gazella* and *O. taurus*, which represent the ancestral cephalic horn morphology (Fig. 2A and B), and *O. sagittarius*, which represents a derived cephalic horn morphology and a reversal in the sexual dimorphism of the posterior cephalic horn (Fig. 2C). We then proceeded with subsequent functional analyses in *O. sagittarius* and one of the ancestral proxy species, *O. taurus*. Four salient results emerged.

3.1. Genomic rearrangement of the Hox cluster in a species with derived horn morphology

We used a reciprocal BLAST approach to identify *Hox* gene orthologs in three horned dung beetle species for which sequenced genomes with chromosome level resolution are available: *O. sagittarius, O. taurus*, and *D. gazella*. Specifically, we targeted the eight canonical insect *Hox* genes that have retained their ancestral function in regional body identity specification during early embryogenesis: *lab, pb, Dfd, Scr, Antp, Ubx, abdA*, and *AbdB*. This approach revealed an intact cluster with exactly one ortholog of each *Hox* gene in the expected 5′ to 3’ order in *D. gazella*, although the coding sequence of *labial* was found to be inverted relative to the orientation of the rest of the cluster (Fig. 2D–Supplementary Table 1). On the orthologous chromosome in *O. taurus*, each Hox gene was found in the expected order, but one large split over 4 Mb in length was detected separating *Ot-lab* from *Ot-pb*.

In the *O. sagittarius* genome, we also uncovered a set of exactly one ortholog per Hox gene on the chromosome largely syntenic to those containing the other dung beetle Hox clusters (Fig. 2D). However, in this genome the canonical order of the cluster diverges (Fig. 2E). Specifically, *Os-lab* is the only gene retaining a central location on the chromosome, while the rest of the cluster now appears in a locus over 9 Mb away near the 5’ end of the chromosome. We tentatively interpret these data to indicate that the *Os-pb – Os-AbdB* section of the *Hox* cluster has

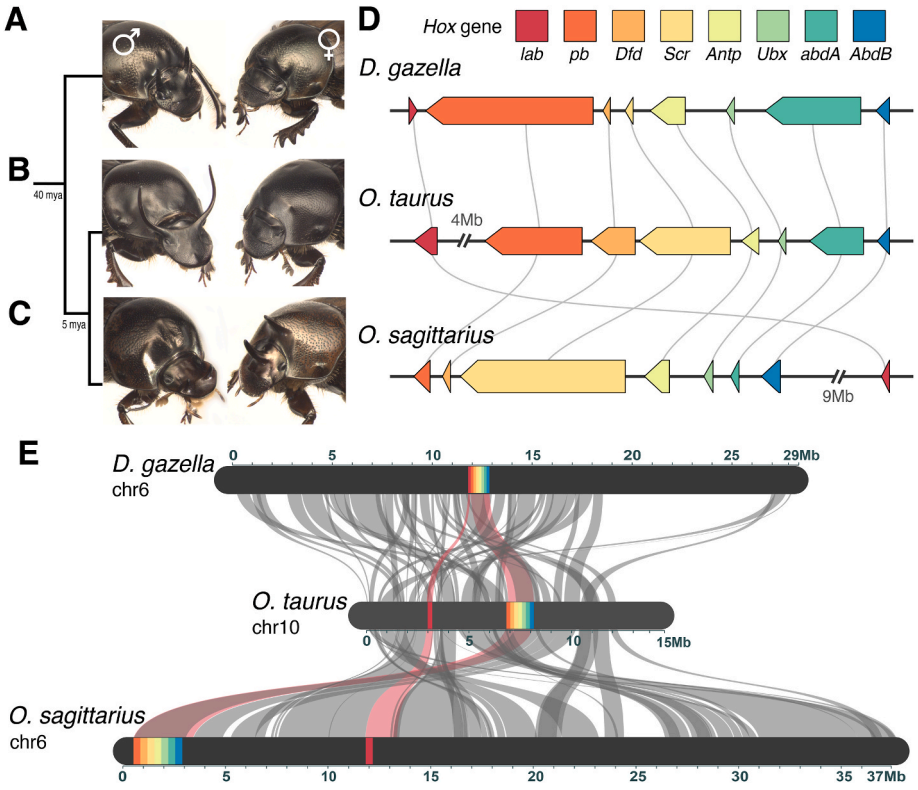

Fig. 2. Genomic rearrangement of the *Hox* cluster in a dung beetle species with derived cephalic horn morphology. Onthophagine dung beetles possess evolutionarily novel and highly diversified head horns. (A) *D. gazella* males possess relatively modest paired posterior horns while females are hornless, whereas (B) *O. taurus* males possess greatly exaggerated paired posterior horns while females are, once again, hornless. (C) In contrast, *O. sagittarius* males are hornless in the posterior head, yet exhibit a novel pair of small anterior horns, while females develop a single medial posterior horn on the head (as well as a medial horn emanating from the prothorax not investigated in the present study). (D) Genomic collinearity of the *Hox* cluster is conserved in *D. gazella* and *O. taurus* but derived in *O. sagittarius* with the ancestrally posterior end of the cluster (*Os-pb* to *Os-AbdB*) absent from its normal location, now instead translocated 9 Mb anterior to *Os-lab* on the same chromosome. Relative gene lengths are represented accurately within but not across genomes in this panel. (E) The chromosomes containing the *Hox* clusters show large blocks of synteny across their length, albeit showing a variety of internal translocations (grey bars), with synteny of *Hox* genes (colored boxes) highlighted as red bars. (For interpretation of the references to color in this figure legend, the reader is referred to the Web version of this article.)

translocated, however due to the occurrence of several other internal translocations on this chromosome across the genus there remains the possibility that more complicated rearrangement scenarios may have occurred in the evolutionary history of this chromosome. Analysis of the collinearity of neighboring and intervening genes suggests that a large split occurred first in the ancestral *Onthophagus* lineage, before the rearrangement specific to *O. sagittarius* (Fig. S1).

To validate this finding and rule out that this arrangement could be an artefact of the genome assembly process, we returned to the contigs generated through PacBio long-read sequencing to assess cluster configuration on the pre-assembly reads. To do so, we generated a custom BLAST database comprised of the complete set of long-read contigs and performed BLAST queries for each *O. sagittarius Hox* gene. In doing so, we confirmed that a single long-read contig contained the entire modified *Hox* cluster, including the new location of the *Os-pb – Os-AbdB* cluster, the 9 Mb intervening stretch, and *Os-lab* (Supplementary Table 2). This result supports the finding that this derived rearrangement is not an artefact of the genome assembly pipeline and instead reflects a novel translocation within the cluster potentially unique to the *O. sagittarius* genome.

3.2. *O. sagittarius maintains canonical Hox expression during embryogenesis*

With the analyses described above indicating a rearrangement of the *Hox* cluster in *O. sagittarius*, we sought to assess whether *Os-labial* retained its canonical segment-restricted expression during embryonic development. To do so we used *in situ* HCR targeting *Os-lab* in embryos roughly 24 h after egg laying (AEL) - to capture embryonic segments prior to the morphogenetic processes described by the bend-and-zipper model - and roughly 72 h AEL, to capture pre-hatchling morphology after these morphogenetic processes have occurred (Fig. 3A). We also targeted *Os-proboscipedia* in the same experiment as a positive control, since this gene has retained its close contiguity with the rest of the Hox cluster in the *O. sagittarius* genome and thus can be predicted to have retained ancestral expression and function.

Staining 24h AEL embryos revealed *Os-lab* signal within the intercalary segment, i.e. the second of the serially homologous segments, posterior to the antennal region, and thus a pattern typical for holometabolous insects (Fig. 3B). As such, the *labial* expression domain closely resembles many aspects of early embryonic *lab* staining reported in *T. castaneum* (Posnien and Bucher, 2010); specifically, in both the flour beetle and the dung beetle, early expression of labial turns on in a stripe bordering the antennal segment, with larger circular domains along the midline trailing into a narrow band laterally. Lateral expression in the dung beetle reported here extends perhaps more posteriorly than in *T. castaneum*, however it is worth noting that precise stage matching during embryonic development between these taxa is currently not available, thus precluding more precise comparisons. Despite several attempts we were, however, unable to capture *Os-pb* staining at the same timepoint, potentially due to conserved temporal collinearity wherein *labial* expression appears prior to any subsequent *Hox* expression.

In contrast, staining in 72 h AEL embryos revealed signal for both *Os-lab* and *Os-pb*. At this developmental stage, the morphogenetic processes described by the bend-and-zipper model are complete and the morphology is now representative of the future larva. Here, *Os-lab* expression was observed dorsally to the mouthparts, posterior to the antenna, and restricted to two distinct lateral rather than one contiguous head region (Fig. 3C). *Os-pb* expression in turn was observed in the segments bearing the maxillary and labial mouthparts, now positioned ventrally in relation to the presumed intercalary segment (Fig. 3C). These results are thus consistent with a conservation of canonical segment patterning by *Os-lab* and *Os-pb*, as well as being qualitatively consistent with the posteriorly and dorsally-restricted expression data published in prior work (Linz and Moczek, 2020). We are unaware of other examples in the literature where pre-hatchling stage *labial* expression patterns have been reported to allow direct comparisons, so it

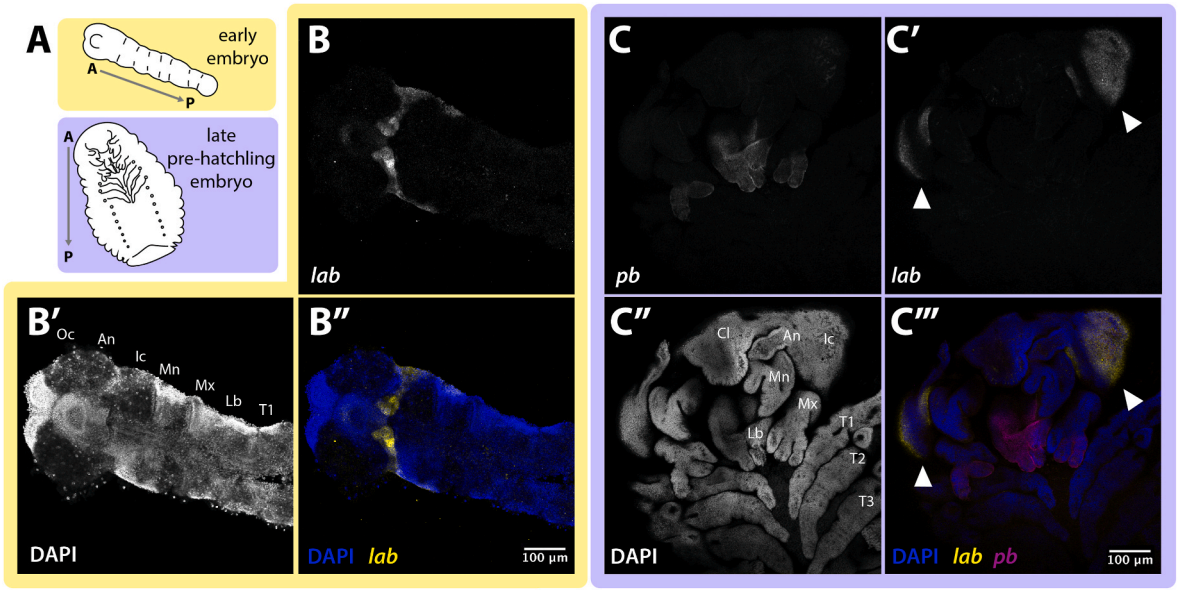

Fig. 3. Canonical *lab* and *pb* expression patterns are maintained despite genomic rearrangement in *O. sagittarius*. Representative diagrams of developmental stages of embryos used for *in situ* HCR staining (A). Yellow outlining (B) indicates data from the early embryonic stage and purple outlining (C) indicates data from the late embryonic stage. In an early *O. sagittarius* embryo approximately 24h after egg laying (AEL) shown dorsally, HCR staining of *lab* (B) co-stained with DAPI (B′), shows typical expression pattern in the intercalary segment. Multichannel image shown in B′′. In an older, pre-hatchling stage *O. sagittarius* embryo shown ventrally, HCR staining for *pb* (C) was performed alongside co-staining for *lab* (C′) and DAPI (C″). Multichannel image shown in panel C‴.Staining at this stage confirms that *pb* is expressed in the expected segments which bear the maxillary and labial feeding appendages; *lab* expression at this stage appears bilaterally in the pre-hatchling head (white arrowheads). Segment abbreviations: Cl – clypeolabral; Oc – ocular; An – antennal; Ic – intercalary; Mn – mandibular; Mx – maxillary; Lb – labial; T1-prothorax; T2 – mesothorax; T3 – metathorax. (For interpretation of the references to color in this figure legend, the reader is referred to the Web version of this article.)

is unclear whether the bilateral expression domains are representative of broader groups of insects or is unique to Scarabaeidae.

3.3. Ventral effects of anterior Hox gene knockdown in horned dung beetles

Next, we analyzed the functions of *lab, pb*, and *Dfd* individually and in combination using larval RNAi in both *O. taurus* (conserved cluster arrangement) and *O. sagittarius* (derived cluster configuration). We predicted that if anterior Hox gene functions are conserved in these species, then RNAi targeting *pb* and *Dfd* – but not *lab* – should recapitulate homeotic transformations of ventral mouthparts well described across diverse insects (Hughes and Kaufman, 2000; Smith and Jockusch, 2014; Zhang et al., 2020). Furthermore, we predicted that RNAi-mediated transcript depletion of any of our three target genes should not affect *dorsal* head patterning in line with the assumption that this body region is not thought to be instructed by *Hox* gene input. Our findings match the first, but diverge from the second prediction.

Specifically, RNAi-mediated transcript depletion of *Os-lab* and *Ot-lab* did not result in homeotic mouthpart transformations, matching predictions from previous work which established that the intercalary segment does not contribute to gnathal appendage formation in insects (Fig. 4D and E). Also as predicted, *Os-pb* and *Ot-pb* RNAi animals exhibited a homeotic transformation of both maxillary palps and labial palps toward leg phenotypes, evidenced by the increased size of the proximal palpomeres, the decrease in size of the distal palpomeres, and the appearance of long sensory bristles on the proximal palpomeres, with particularly well-developed ectopic femurs borne by the maxillary palps (Fig. 4F and G). *Os-Dfd* and *Ot-Dfd* RNAi animals also exhibited a knockdown phenotype in the maxilla as expected, specifically a rounding of the everted corners of the base of the maxillary galea (Fig. 4H and I), although no deformation was detected in the mandibles from *Dfd* RNAi alone, diverging from findings in *Tribolium* (Fig. S2B).

Double knockdown of *pb* and *Dfd* in *O. sagittarius* and *O. taurus* resulted in a new set of homeotic transformations: labial palps transformed to express leg identity while maxillary palps acquired antennal identity, as evidenced by the enlargement of the medial and distal palpomeres and the appearance of densely packed, short sensory bristles. (Fig. 4J and K). The double knockdown treatment led to a deformation of the mandibles, specifically the appearance of ectopic bristles on the molar region (Fig. S2C). Further, triple knockdown of *lab* + *pb* + *Dfd* in *O. sagittarius* and *O. taurus* recapitulated the ventral homeotic transformations that resulted from the double knockdown treatment (Fig. 4L–M, Fig. S2D). Collectively, the nature and extent of mouthpart transformations observed here thus largely match those reported previously in *Tribolium* beetles (Smith and Jockusch, 2014), validate our RNAi methodology in dung beetles, and indicate a high degree of conservation of *Hox* patterning function in the ventral head during the metamorphic transition in Coleoptera.

3.4. Dorsal effects of anterior Hox gene knockdown in horned dung beetles

Likewise consistent with our initial predictions, two of our three *Hox* gene knockdowns failed to alter *dorsal* head formation. Specifically, *Os-pb* and *Ot-pb* RNAi animals did not exhibit any dorsal head patterning alterations within or outside horn-bearing regions or the corresponding hornless regions in alternate sexes (Fig. S3B). Similarly, *Os-Dfd* and *Ot-Dfd RNAi* animals did not exhibit any dorsal head patterning defects (Fig. S3C), nor did animals obtained from the *pb* and *Dfd* double knockdown treatments (Fig. S3D).

However, our *lab* RNAi experiment resulted in an unexpected dorsal head phenotype in both *O. taurus* and *O. sagittarius*. In particular, while *lab* RNAi animals did not reveal any obvious alterations with respect to horn presence, position, size, or shape (Fig. 5A and B), *lab* RNAi treatment did result in a bilateral patterning defect in the posterior-most dorsal head of both species. Specifically, *lab* RNAi resulted in a deformation of the *tempora* (or *temples*; *sensu* Steinman and Zombori, 2012; Lawrence and Slipinski, 2013), which in wildtype and control-injected individuals represent the typically conspicuously everted dorsal postero-lateral corners of the head located behind the eyes. *lab* RNAi individuals, in contrast, lacked everted tempora in males and females of both species, resulting instead in a conspicuous narrowing of the dorsal posterior head (Fig. 5C and D).

Lastly, triple knockdown of *lab* + *pb* + *Dfd in O. sagittarius* resulted in a combination of dorsal and ventral phenotypes seen in single gene RNAi treatments, with animals exhibiting the bilateral reduction and rounding of temples in addition to mouthpart transformations (Fig. S3E). In partial contrast, triple knockdown of *lab* + *pb* + *Dfd* in *O. taurus* only recapitulated the ventral homeotic transformations, and did not result in animals exhibiting rounded corners in the dorsal posterior head (Fig. S3F).

3.5. Ablation-based fate mapping confirms correspondence between labial expression in larvae and adult labRNAi phenotypes

The work presented above established first, the expression pattern of *Os-lab* in the embryo, and second, the loss of adult temples following *lab* RNAi in larvae. We additionally attempted to assay *Os-lab* expression in the premetamorphic larval head but were not able to generate robust data due to limitations of the whole-mount *in situ* HCR technique. We therefore proceeded under the assumption that the larval expression pattern would roughly correspond to the *labial*-expressing cells seen in the pre-hatchling head (Fig. 3), although there are examples in the literature that *Hox* expression patterns can be dynamic over time (Gąsiorowski and Hejnol, 2019). However, given that published RNAseq data showed *labial* expression spatially restricted to the dorsal head and enriched in the lateral head relative to the medial head (Linz and Moczek, 2020), we feel there is evidence that the expression pattern is maintained to some degree throughout juvenile development. Therefore, to more explicitly establish a link between the early gene expression pattern to the post-metamorphic RNAi phenotype, we used an ablation-based fate mapping approach to remove head epithelial cells in *O. taurus* and *O. sagittarius* larvae prior to their metamorphic transition and assayed the resulting adult phenotypes (as in Busey et al., 2016).

With the ablation approach, we focused on three separate regions of the posterior dorsal head, targeting cells on the right side of the head of each treated larvae and leaving the left side of the head untreated to serve as a negative control (Fig. 6A, Supplementary Table 4). Note that for ease of viewing of the temple region, we took advantage of the high nutrition sensitivity of horn development in *O. taurus* to rear smaller-sized males, such that their correspondingly smaller head horns would not obscure viewing of the *tempora* from a dorsal perspective.

Ablation targeting region 1, the most lateral region, resulted in unilateral loss of the right compound eye in both species, while targeting region 3, closest to the posterior dorsal midline of the head, resulted in no observable morphological defects (Fig. S4). Ablation targeting region 2 resulted in unilateral rounding or flattening of the normally everted right temple of the cuticular vertex of the posterior head in both species, thus phenocopying *lab* RNAi results. Note that ablation of region 2 in *O. taurus* (but not the larger *O. sagittarius*) also consistently eliminated the right adult compound eye. This suggests that in this species the larval intercalary epithelium and the larval ocular primordia are in such close spatial proximity that the relatively coarse-grained ablation approach taken here could not target region 2 in *O. taurus* without also affecting region 1 due to the much smaller size of *O. taurus* larvae.

4. Discussion

Motivated by preliminary data documenting unexpected *Hox* gene expression in the dorsal heads of beetle larvae, we investigated the

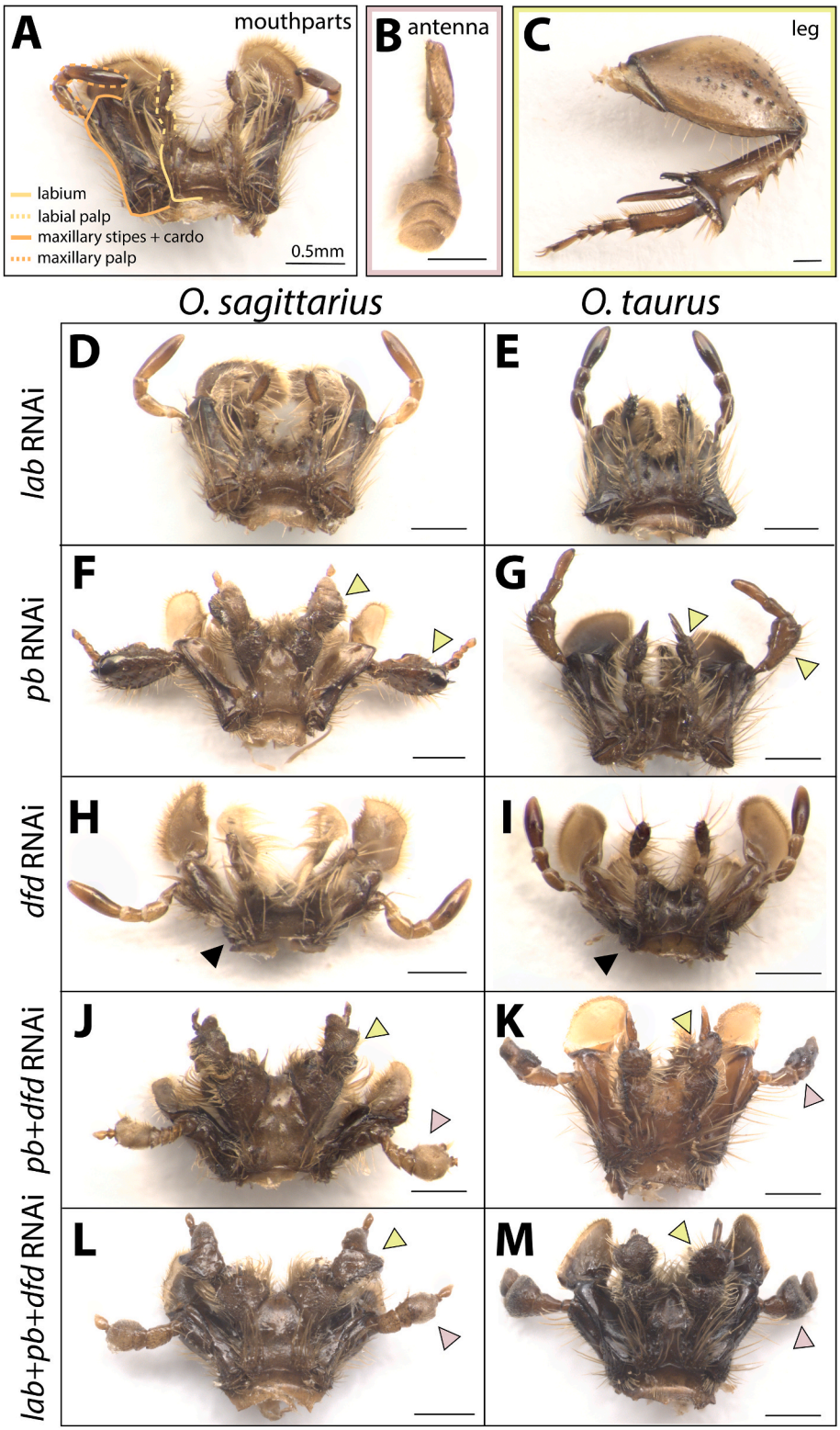

Fig. 4. Homeotic transformations of adult mouthparts following larval *Hox* RNAi in dung beetles mirror those described for other beetle taxa. Buffer-injected control *O. sagittarius* illustrating wildtype appendages: mouthparts derived from the maxillary and labial segments (A) antenna (B), and mesothoracic leg (C). *Hox* gene knockdown via RNAi in *O. sagittarius* and *O. taurus* results in a range of homeotic transformations (D to M). *Os-lab* RNAi (D) and *Ot-lab* RNAi (E) did not result in changes to mouthpart morphology. *Os-pb* RNAi (F) and *Ot-pb* RNAi (G) resulted in transformation of the maxillary palps and labial palps to legs, indicated by the increased size of the proximal palpomeres, the decrease in size of the distal palpomeres, and the appearance of sensory bristles on the proximal palpomeres (green arrowheads in F, G). *Os-dfd* RNAi (H) and *Ot-dfd* RNAi (I) resulted in deformation of the maxillary cardo and stipes, indicated by the smaller, rounded shape of the base (black arrowheads in H, I). Double RNAi of *pb* + *dfd* in *O. sagittarius* (J) and *O. taurus* (K) resulted in transformation of the maxillary palps to antennae (pink arrowheads in J, K) and the labial palps to legs (green arrowheads in J, K). Triple RNAi knockdown of *lab* + *pb* + *dfd* in *O. sagittarius* (L) and *O. taurus* (M) also resulted in transformation of the maxillary palps to antennae (pink arrowheads in L, M) and the labial palps to legs (green arrowheads in L, M). (For interpretation of the references to color in this figure legend, the reader is referred to the Web version of this article.)

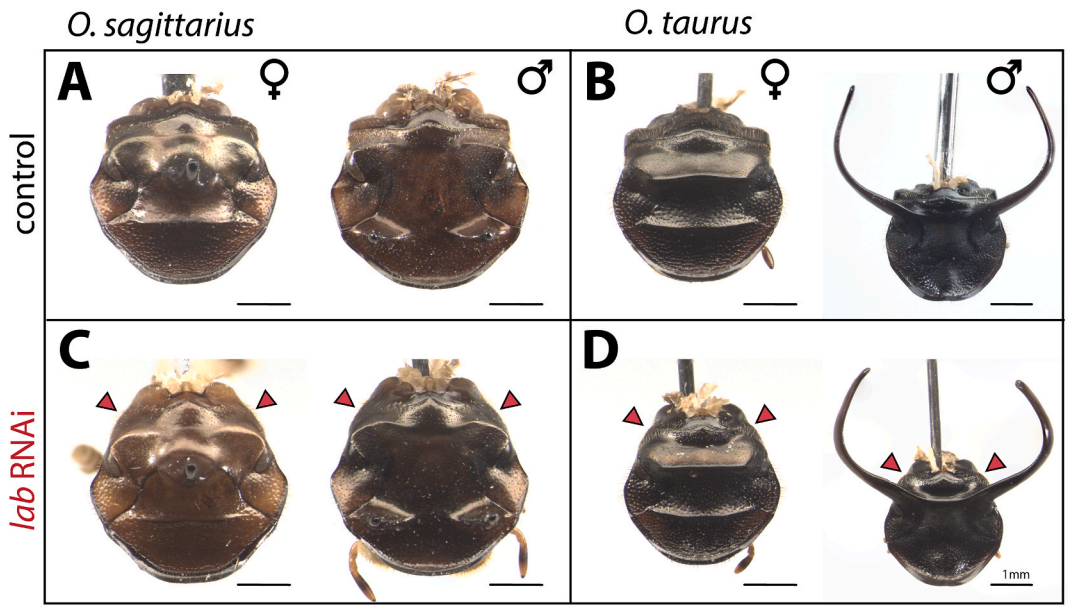

Fig. 5. *lab* RNAi results in the loss of the tempora located in the dorsal posterior head. Dissected heads of buffer-injected control beetles illustrating normal dorsal head morphology for *O. sagittarius* (A) and *O. taurus* (B). *Os-lab* RNAi did not affect horn presence, positioning, size, or shape in male or female adults, but did result in the bilateral deformation of the posterolateral tempora (temples) in both sexes (C, red arrowheads). *Ot-lab* RNAi similarly did not affect horn presence, positioning, size, or shape in males, but again resulted in bilateral deformation of the temples in both sexes (D, red arrowheads). (For interpretation of the references to color in this figure legend, the reader is referred to the Web version of this article.)

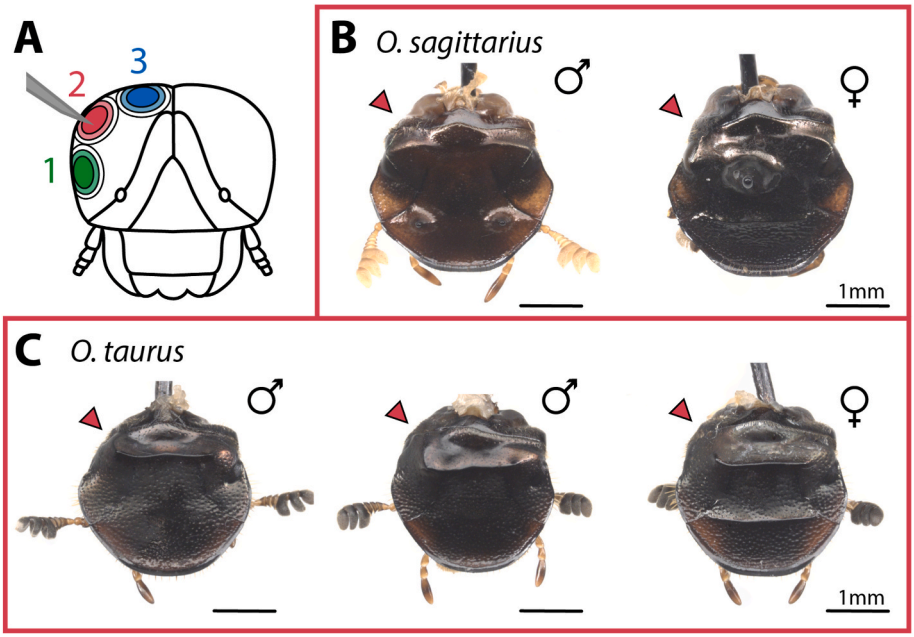

Fig. 6. Ablation-based fate mapping of the larval head recapitulates loss of temples seen in *labial* RNAi phenotypes. Diagram of the larval head regions that were unilaterally targeted through ablation-based fate mapping (A). Ablation of region 2 resulted in a flattening of the posterolateral tempus, phenocopying the result of *lab* RNAi in *O. sagittarius* adults (B) and *O. taurus* adults (C; two representative male individuals are shown). Phenotypes resulting from ablation of regions 1 and 3 can be found in Supplementary Fig. 4.

genomic *Hox* content and arrangement in multiple species of horned dung beetles. We then assessed embryonic *Hox* expression patterns and tested for the potential function of anterior *Hox* genes *labial, proboscipedia,* and *Deformed* in establishing the segmental boundaries of the adult beetle head and in patterning their highly diversified, evolutionarily novel cephalic horns. Below we discuss the most important implications of our results for our understanding of the development, evolution, and diversification of the insect head.

4.1. Onthophagus sagittarius labial is translocated outside the Hox cluster yet exhibits conserved intercalary segment expression

Our reciprocal BLAST approach, secondary validation of cluster contiguity on PacBio sequences, and synteny mapping indicated that the canonical insect *Hox* cluster is intact with a full complement of genes in *D. gazella*. In partial contrast, while a similarly complete complement of Hox genes present on the orthologous chromosome was uncovered in

O. taurus, a 4 MB split was detected separating *Ot-lab* from *Ot-pb* and the rest of the cluster. The cluster arrangement in the third species, *O. sagittarius,* was more unexpected. Here, the majority of the posterior cluster (from *Os-pb* to *Os-AbdB*) is translocated ~8 MB anteriorly on the chromosome, with the ancestrally most anterior gene *Os-lab* alone maintaining a more central location (Fig. 2). The conditions and mechanisms that may have led to this translocation remain unclear, however, recent comparative genomic analyses of this clade have uncovered a massive degree of transposable element expansion across the *O. sagittarius* genome (Davidson and Moczek, 2024), indicating that transposable element insertions and subsequent inversions could be one potential mechanism underlying this cluster rearrangement in this species. Furthermore, we hypothesize that the ancestral split separating *lab* and *pb* in the *Onthophagus* lineage allowed *Os-lab* to escape such tight linkage with the remaining cluster, providing more opportunity for repositioning to occur.

While the *Hox* gene cluster is known for its deeply conserved collinearity, phenomena including cluster splits, inversions, and gene translocations are not wholly uncommon (Lemons and McGinnis, 2006; Mulhair and Holland, 2022). A broad comparative study across insect orders performed by Mulhair and Holland (2022) indicated that genomic splits among the Hox genes are most common among the anterior Hox genes *lab, pb,* and *Dfd*, a finding corroborated here by the evidence of a split in the cluster predating the split between the *O. taurus* and *O. sagittarius* lineages. Furthermore, a study of seven species within the genus *Drosophila* established that none of the species exhibited the single closely linked complex that is putatively ancestral for the genus and seen in other Diptera, each of them instead possessing one or more major splits (Negre and Ruiz, 2007). Specifically, two of the major cluster splits were dated to have occurred between 63 and 43 million years ago, with one more recent split having occurred between 30 and 20 million years ago. Other panarthropod taxa such as the tardigrades have even sustained major *Hox* gene loss, retaining only five of the eight body patterning genes (Smith et al., 2016). Translocations are not seen quite as frequently as cluster splits, but are still documented across various insect orders. For example, the translocation of *lab* past the end of the remaining Hox cluster, matching the data reported here in *O. sagittarius*, is seen in most Lepidoptera (Mulhair and Holland, 2022). Our results here contribute to this larger body of work and document an exceptionally recent cluster translocation, with phylogenetic estimates dating the most recent common ancestor of *O.sagittarius* and *O. taurus* to within the last 5 million years (Davidson and Moczek, 2024).

Furthermore, experimental manipulations in vertebrates have shown that the presence of enhancer sequences within the endogenous cluster orientation is crucial for proper regulation of Hox gene function (Tschopp and Duboule, 2011; Tschopp et al., 2011). Experimentally generated inversions and translocations separating normally linked enhancers from their target Hox genes phenocopy deletions of those coding sequences, indicating that evolutionary separation of a Hox gene from its ancestral regulatory landscape may be sufficient to alter its function. However, the vertebrate Hox cluster displays an unusual degree of compactness, and these conclusions may not hold for other taxa such as arthropods with less compact Hox clusters.

Given that the derived cluster arrangement in *O. sagittarius* specifically affected *labial,* i.e. the *Hox* gene expressed most anteriorly, and considering that this species possesses a highly derived head horn morphology relative to the ancestral state for this clade (Emlen et al., 2005), we next pursued expression and function analyses of the anterior-most Hox genes *labial* and *proboscipedia* to assess the possible functional significance of this derived cluster configuration. Specifically, we sought to assess whether the genomic rearrangement could underlie a derived function in regulating the patterning of the *O. sagittarius* head and/or the cephalic horns contained therein. Using *in situ* hybridization chain reaction, we found *lab* and *pb* expression patterns to be largely conserved: specifically, we detected *Os-labial* expression during early embryogenesis within the presumptive intercalary segment posterior to the non-segmental ocular region. (Fig. 3B). *Os-proboscipedia* in turn was expressed – again following expectations – in the segments bearing the maxillary and labial mouthparts (Fig. 3C). In later pre-hatchling embryos, *Os-lab* expression was detected in two distinct lateral regions of the head, a finding congruent with the RNAseq expression data found dorsalaterally, but without other stage-matched comparative data points in the literature that we are aware of (Fig. 3C). Altogether, the expression data did not support our hypothesis that Hox cluster rearrangement could underlie a change in Hox gene regulation and thus expression.

4.2. *RNAi targeting anterior Hox genes transforms mouthparts as expected but does not alter head horn formation*

Famously, Hox gene manipulations result in homeotic body segment transformations, including the corresponding appendages generated by each segment (Carroll, 1995). The original studies in *Drosophila* revealed a functional hierarchy in the patterning mechanism of the Hox genes termed *posterior prevalence.* This phenomenon describes a pattern wherein ectopic expression of a posterior Hox gene in an anterior segment overrides normal segment identity, and where the attenuation of posterior Hox expression allows more anterior segment identities to become de-repressed (Lewis, 1978; Yao et al., 1999). This phenomenon is controlled on a molecular level by the hierarchical dominance of posterior Hox genes over the function of more anterior Hox genes, and is achieved by a diverse set of mechanisms including mutual transcriptional repression between co-expressed Hox genes (Hafen et al., 1984; Carroll et al., 1986).

Data from embryonic studies in *T. castaneum* established that Hox genes generally repress antennal identity throughout the more posterior gnathos and trunk (Brown et al., 2002). More recently, Smith and Jockusch (2014) assessed the roles of *Hox* identity specification during metamorphosis and documented the mouthpart transformations that occur in adult *T. castaneum* after larval *Hox* RNAi. These data led us to predict that *Hox* manipulations knocking down *pb* and *Dfd* in *Onthophagus* beetles would result in a matching set of homeotic transformations of the mouthparts; in contrast, manipulations targeting *lab*, which specifies the appendage-less intercalary segment, have not been documented to cause homeotic phenotypes in adults (Smith and Jockusch, 2014).

Our data closely matched these prior results (Fig. 4). RNAi targeting *lab* did not generate any mouthpart transformations, as expected, while attenuation of *pb* expression resulted in the transformation of two gnathal appendages, the maxillary and labial palps, to express leg identity, although the phenotypes here did not represent complete transformations of all palpomeres. Instead, we observed obvious transformations of the proximal palpomeres toward femur-like morphology, and while the medial and distal palpomeres displayed dramatic differences from their typical morphology they did not display complete transformations to tibial and tarsal morphology. Based on the logic of posterior prevalence, these phenotypes are explained by the anterior migration of Scr and Antp expression, two genes which normally regulate appendage identity in the thorax, now specifying thoracic identity in gnathal segments (Abzhanov et al., 2001). Attenuation of *Dfd* expression in turn resulted in deformations of the base of the maxilla and mandible, but not in homeotic transformations. This phenotype is likely due to partial maintenance of gnathal segment identity by *pb* expression that is retained in the gnathal segments (Brown et al., 2002). Double knockdown of *pb* and *Dfd* resulted in the transformation once again of labial palps to legs, but of maxillary palps into antennae; this is likely due in part to anterior migration of *Scr* and *Antp*, along with new posterior expression of antennal specification genes in the anterior head, in line with findings in other insects illustrating that antennal identity is the default state that will be expressed in absence of any *Hox* gene expression (Brown et al., 2002). Taken together, our suite of results provides support for a high degree of conservation across Coleoptera for the regulation of gnathal segment patterning by *Hox* genes during

metamorphosis.

As mentioned previously, Hox genes are most famous for the homeotic transformations that they induce when their expression is manipulated. The transformations of the ventral mouthparts described above are two such examples of these dramatic phenotypes wherein the identity of the segment and its appendages changes. In non-insect arthropod lineages, the head region homologous to the intercalary segment – the tritocerebral segment – has retained a pair of appendages, and *labial* RNAi in these taxa results in traditional homeotic transformations. Specifically, in Opiliones (harvestmen), *lab* RNAi transforms the pedipalp appendages of the tritocerebral segment into chelicera, the appendages typically found on the more anterior deutocerebral segment (Gainett et al., 2023). Intriguingly, in Arachnida (spiders), loss of *labial* was shown to cause complete appendage loss, where the tritocerebral segment of the prosoma still formed but the pedipalp appendages were absent or dramatically reduced and increased cell death was reported in the tritocerebral segment of the head (Pechmann et al., 2015). Tissue maintenance may be a broadly conserved function of labial in arthropods, as increased cell death after lab RNAi has been documented in Tribolium as well (Schaeper et al., 2010).

In contrast, the intercalary segment of insects lacks appendages, and thus the phenotypes resulting from *labial* knockdown across insect orders are more nuanced, including for example a regional deletion of the bristles normally found on the lateral gena of the head, reported in *Tribolium castaneum* larvae following parental RNAi (Posnien and Bucher, 2010). In the fruit fly, *labial* malfunction during larval development causes a failure of head involution, a phenotype largely unique to Dipterans, as this order displays a highly derived mode of head development (Merrill et al., 1989). Importantly, despite the larval phenotype resulting from parental *lab* RNAi in *Tribolium,* no adult phenotype was reported after RNAi treatment of juveniles (Smith and Jockusch, 2014). Additionally, maternal and zygotic RNAi approaches in Oncopeltus, a hemipteran species, failed to reveal any function of labial in head patterning (Angelini et al., 2005). Given this lack of adult phenotypes reported in other insects, and based on the predictions of the bend-and-zipper model, we hypothesized that *lab* RNAi should not affect the adult dorsal head of dung beetles.

In addition to assessing the ventral mouthpart transformations described above, we sought to test whether *Hox* RNAi might also result in morphological effects on the cephalic horns in the dorsal head due to the detectable dorsal expression of these genes during the early stages of metamorphosis (Linz and Moczek, 2020) and the previously unknown boundaries of the intercalary segment in the post-metamorphic head. However, larval *Hox* RNAi treatments did not result in any cephalic horn patterning defects, in either the species with canonical or derived *Hox* cluster arrangements. Across multiple distinct horn morphologies (paired lateral posterior horns in male *O. taurus*, a single medial posterior horn in female *O. sagittarius*, and paired anterior horns in male *O. sagittarius)*, *Hox* RNAi treatments did not affect horn presence, positioning, number, size or shape. Instead, these results are consistent with earlier ablation fate mapping findings (Busey et al., 2016) that suggested that the diversity of cephalic horns found in *O. taurus* and *O. sagittarius* do in fact derive solely from the non-segmental ocular region of the head rather than any segmentally derived tissues.

4.3. Labial knockdown and ablation-based fate mapping approaches resolve beetle head segment boundaries between larval and adult stages

Although our RNAi treatments targeting *lab* did not affect horn forming regions, this approach did nevertheless reveal an unexpected morphological patterning deffect in the dorsal head outside horn forming regions. In *Os-lab* and *Ot-lab* RNAi treatments, males and females of both species exhibited a bilateral reduction and rounding of the posterolateral temples, which are positioned behind the compound eyes anterior to the cephalic articulation with the prothorax (Fig. 5). Importantly, these regions qualitatively correspond to the *Os-lab* expression pattern observed in the late embryonic stages (Fig. 3), as well as the strong lateral expression detected in transcriptomic studies at the prepupal stage in *O. taurus* (Linz and Moczek, 2020). Interestingly, cell death following lab RNAi has been reported in Tribolium and other arthropods, which could be a plausible mechanism underlying the reduction of the temples reported here (Schaeper et al., 2010; Pechmann et al.,2015).

Along with the data reported from earlier life stages, we take these findings to suggest that in Onthophagine beetles, the intercalary segment and corresponding *labial* expression are present as expected in the early, flat embryo, then – in addition to the morphogenetic processes described by the bend-and-zipper model - the intercalary segment bifurcates into two lateral domains, resulting by the end of larval head morphogenesis in the intercalary segment regions being positioned posterior to each antennal segment and dorsally to the mouthpart-bearing segments, in line with the RNAi phenotypes documented in this study. As such, our results are qualitatively congruent with a regional deletion reported in *T. castaneum* larvae following parental RNAi (Posnien and Bucher, 2010), and we are unaware of any comparative gene expression data in the literature at this specific pre-hatchling timepoint. Even though the proportion of the head affected by this regional deletion in T. castaneum appears smaller than the proportion of the lateral head showing *lab* staining in *O. sagittarius*, we believe these differences are in relative size rather than location. Based on previous RNAseq data from Onthophagine heads, we thus propose that the bilateral domains of *lab* expression are maintained throughout larval development and through metamorphosis into the derived, flattened adult head morphology characteristic of Onthophagine beetles; the bilateral defects seen in the dorsal heads after *lab* RNAi are also congruent with this interpretation. However, previous studies in *T. castaneum* failed to find any effect of larval *lab* RNAi on *adult* head structures (Smith and Jockusch, 2014). Therefore, to further assess the relationship between juvenile *lab* expression data to the *lab*RNAi phenotypes observed in *Onthophagus* adults, we performed ablation-based fate mapping during larval development. The fate mapping data confirmed that ablation of a targeted region of the posterolateral larval head affects the adult head in ways similar to those induced by larval *lab* RNAi (Fig. 6). Taken together, the data generated here begin to establish correspondence between embryonic, juvenile, and adult head segments of onthophagine beetles (Fig. 7). These findings have a range of possible implications, which we will discuss in turn.

One possible interpretation of these data is that these phenotypes continue to reflect a reliable fate map for the intercalary segment throughout embryonic, juvenile, and adult stages of *Onthophagus* head morphogenesis. If so, this interpretation would imply that the anterior-dorsal closure motion proposed by the bend-and-zipper model may hold for the majority - but not entirety - of the dorsal *Onthophagus* head. Rather than extending fully across the mediolateral axis covering the intercalary, maxillary, mandibular, and labial segments positioned on the ventral side of the head, as proposed earlier, our findings raise the possibility that the dorsal closure of the ocular region may extend all the way to the prothoracic segment only in the medial head. If so, the bilateral adult *Onthophagus* genae may derive instead from the intercalary segment that has separated and migrated bilaterally to form the posterolateral head, matching data reported in larval *Tribolium* by Posnien and Bucher (2010). While this interpretation would seem at odds with a lack of phenotype reported in adult *Tribolium* following larval *lab*RNAi, this discrepancy could be accounted for by the fact that the morphology of the adult *Tribolium* gena is more flattened, simplified by comparison, and does not generate any protrusions such as the scarab temples. Thus any effect of *lab*RNAi may have been too subtle to detect, as neighboring head epithelial cells may have been able to proliferate and compensate for the deletion of the intercalary segment, producing a morphology roughly equivalent to that of wildtype in the process.

A similar scenario that we cannot reject based on current data is that the intercalary *Onthophagus* segment bifurcates and migrates bilaterally

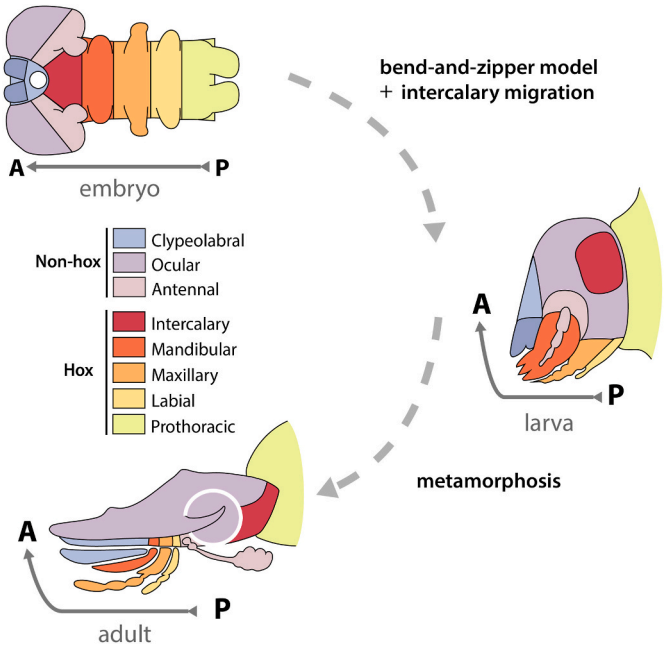

Fig. 7. Pregnathal segment boundaries throughout Onthophagine development. *lab* expression data, RNAi phenotypes, and ablation fate mapping results suggest that the posterolateral temples of the vertex of the adult beetle head derive from the intercalary segment, while the remaining gnathal segments contribute only to ventral mouthpart-forming regions.

within the head, yet in adult *Onthophagus* and adult *Tribolium* does *not* contribute to the externally visible genae. The flattening of the temples seen after *lab*RNAi could then be explained by the deletion of internal tissue that no longer scaffolds everted temples. This interpretation would again account for the lack of corresponding RNAi phenotypes found in adult *Tribolium*. Alternatively, we cannot fully exclude the hypothesis that evolutionary changes in the timing and/or spatial distribution of *lab* expression and function among beetle families may account for differential presence and absence of adult *lab*RNAi phenotypes. For example, in *Tribolium* larvae the segmental contributions to the head include a lateral contribution of the intercalary segment to the genae. During metamorphosis the ocular and/or antennal regions have been suggested to replace this contribution in *Tribolium,* but may not do so in *Onthophagus,* thereby explaining the absence and presence of adult *lab*RNAi phenotypes, respectively. While the above scenario posits an evolutionary change in *labial* expression across developmental *time*, changes to its *spatial* expression may similarly account for the results presented here. For instance, the domain of *lab* expression may have expanded in *Onthophagus* relative to *Tribolium*, yielding a larger internal and/or external head contribution in the process. Given that the molecular mechanism of mutual transcriptional repression between Hox genes does not limit expansion of labial into the ocular region, this scenario cannot be ruled out. Additionally, there are documented examples of clearly novel Hox expression patterns in the literature, such as the expansion of the *Ubx* domain to the mesothoracic leg in water striders (Khila et al., 2009).

While data at present do not allow us to distinguish between these alternative scenarios described above, collectively, our results document that *labial* functions in patterning the dorsal head in dung beetles, a region previously thought to be derived from the non-segmental *Hox-free* pre-ocular region of the embryo. These data allow for reconciliation of the unexpected *lab* expression data detected in previous work (Linz and Moczek, 2020), by shedding light on the complex processes of adult head morphogenesis in the derived, flattened Onthophagine head morphology. However, this work also established a lack of functional consequences for *pb* RNAi in the dorsal head, indicating that this expression detected in the dorsal head must be latent, or was derived from more internal tissues not reflective of the segmental origin of the local epithelia. Furthermore, these results establish a conservation of general *Hox* patterning function despite an unexpected genomic rearrangement of the cluster in one of three Onthophagine beetles studied and contribute to an understanding of the morphogenetic processes underlying development of the beetle head throughout the life cycle.

In studies on the origin of *prothoracic* horns in beetles, investigation of the *Hox* gene *Scr* was instrumental in uncovering the serial homology of horns on the prothorax and wings on the meso- and metathorax, among other paired bilateral structures on abdominal segments (Hu et al., 2019; Hu and Moczek, 2021). Preliminary RNAseq work and discovery of an unexpected rearrangement of the Hox cluster motivated the consideration of anterior Hox genes as potentially relevant in the origin and diversification of cephalic horns. However, the work here documents that *Hox* regulation has likely not played a role in origin or diversification of cephalic horns, making clear that despite the elegant ecological and behavioral integration of cephalic and prothoracic horns, these two horn types arose through intriguingly distinct evolutionary and developmental mechanisms. Thus, future work must uncover the upstream regulators that enabled the developmental genetic origins of this enigmatic evolutionary novelty.

CRediT authorship contribution statement

Erica M. Nadolski: Writing – review & editing, Writing – original draft, Methodology, Investigation, Funding acquisition, Formal analysis, Conceptualization. **Isabel G. Manley:** Writing – review & editing, Investigation, Formal analysis. **Sukhmani Gill:** Writing – review & editing, Investigation, Formal analysis. **Armin P. Moczek:** Writing – review & editing, Writing – original draft, Supervision, Resources, Funding acquisition, Conceptualization.

Acknowledgements

The authors would like to thank Dr. David Linz for inspiration and assistance with generating figure components, Dr. Eduardo Zattara for assistance with generating the bend-and-zipper model figure, Dr. Phil Davidson for assistance compiling genomic analysis programs, Dr. Frank-Thorsten Krell for assistance in parsing the literature on scarab morphological terminology, and Dr. Andras Kun and the Indiana University Light Microscopy and Imaging Center for providing microscopy expertise and equipment. Comments by Dr. Phil Davidson, Dr. Rebecca Westwick, Dr. Joshua Jones, Kenzie Givens, and two anonymous reviewers greatly improved earlier drafts. This work was supported in part through generous funding from the National Science Foundation [Grant no. 2243725 and 1901680 to APM] and was performed while EMN was funded by the National Institutes of Health [T32-HD049336]. Additional support was provided by the IU Groups Scholars Summer Research Experience to SG.

Appendix A. Supplementary data

Supplementary data to this article can be found online at https://doi.org/10.1016/j.ydbio.2025.07.002.

Data availability

Data will be made available on request.

References

Abzhanov, A., Kaufman, T.C., 1999. Homeotic genes and the arthropod head: expression patterns of the labial, proboscipedia, and deformed genes in crustaceans and insects. Proc. Natl. Acad. Sci. 96 (18), 10224–10229. https://doi.org/10.1073/pnas.96.18.10224.

Abzhanov, A., Holtzman, S., Kaufman, T.C., 2001. The drosophila proboscis is specified by two hox genes, proboscipedia and sex combs reduced, via repression of leg and antennal appendage genes. Development 128 (14), 2803–2814. https://doi.org/10.1242/dev.128.14.2803.

Altschul, SF, Gish, W, Miller, W, Myers, EW, Lipman, DJ, 1990. Basic local alignment search tool. Journal of molecular biology 215 (no 3), 403–410.

Angelini, DR, Liu, PZ, Hughes, CL, Kaufman, TC, 2005. Hox gene function and interaction in the milkweed bug *Oncopeltus fasciatus* (Hemiptera). Developmental Biology 287 (2), 440–445.

Bandi, V., Gutwin, C., 2020. Interactive exploration of genomic conservation. In: Proceedings of the 46th Graphics Interface Conference on Proceedings of Graphics Interface 2020 (GI'20). Canadian Human-Computer Communications Society. Waterloo, CAN.

Brown, S.J., Shippy, T.D., Beeman, R.W., Denell, R.E., 2002. Tribolium hox genes repress antennal development in the gnathos and trunk. Mol. Phylogenet. Evol. 24 (3), 384–387. https://doi.org/10.1016/S1055-7903(02)00205-1.

Busey, H.A., Zattara, E.E., Moczek, A.P., 2016. Conservation, innovation, and bias: embryonic segment boundaries position posterior, but not anterior, head horns in adult beetles. J. Exp. Zool. B Mol. Dev. Evol. 326 (5), 271–279. https://doi.org/10.1002/jez.b.22682.

Carroll, S.B., Laymon, R.A., McCutcheon, M.A., Riley, P.D., Scott, M.P., 1986. The localization and regulation of antennapedia protein expression in drosophilaembryos. Cell 47, 113–122. https://doi.org/10.1016/0092-8674(86)90372-7.

Carroll, S.B., 1995. Homeotic genes and the evolution of arthropods and chordates. Nature 376, 479–485. https://doi.org/10.1038/376479a0.

Cheng, H., Concepcion, G.T., Feng, X., Zhang, H., Li, H., 2021. Haplotype-resolved de novo assembly using phased assembly graphs with hifiasm. Nat. Methods 18, 170–175. https://doi.org/10.1038/s41592-020-01056-5PMID:33526886.

Choi, H.M.T., Schwarzkopf, M., Fornace, M.E., Acharya, A., Artavanis, G., Stegmaier, J., Cunha, A., Pierce, N.A., 2018. Third-generation in situ hybridization chain reaction: multiplexed, quantitative, sensitive, versatile, robust. Development 145 (12), dev165753. https://doi.org/10.1242/dev.165753.

Davidson, P.L., Moczek, A.P., 2024. Genome evolution and divergence in cis-regulatory architecture is associated with condition-responsive development in horned dung beetles. PLoS Genet. 20 (3), e1011165. https://doi.org/10.1371/journal.pgen.1011165.

Emlen, DJ, Marangelo, J, Ball, B, Cunningham, CW, 2005. Diversity in the weapons of sexual selection: horn evolution in the beetle genus *Onthophagus* (Coleoptera: Scarabaeidae). Evolution 59 (5), 1060–1084.

Gainett, G., Klementz, B.C., Blaszczyk, P.O., Bruce, H.S., Patel, N.H., Sharma, P.P., 2023. Dual functions of labial resolve the hox logic of chelicerate head segments. Mol. Biol. Evol. 40 (3), msad037. https://doi.org/10.1093/molbev/msad037.

Gąsiorowski, L., Hejnol, A., 2019. Hox gene expression in postmetamorphic juveniles of the brachiopod Terebratalia transversa. EvoDevo 10 (1), 1. https://doi.org/10.1186/s13227-018-0114-1.

Hafen, E., Levine, M., Gehring, W.J., 1984. Regulation of antennapedia transcript distribution by the bithorax complex in drosophila. Nature 307, 287–289. https://doi.org/10.1038/307287a0.

Hu, Y., Linz, D.M., Moczek, A.P., 2019. Beetle horns evolved from wing serial homologs. Science 366 (6468), 1004–1007. https://doi.org/10.1126/science.aaw2980.

Hu, Y., Moczek, A.P., 2021. Wing serial homologues and the diversification of insect outgrowths: insights from the pupae of scarab beetles. Proc. Biol. Sci. 288 (1943), 20202828. https://doi.org/10.1098/rspb.2020.2828.

Hughes, C.L., Kaufman, T.C., 2000. RNAi analysis of deformed, proboscipedia and sex combs reduced in the milkweed bug oncopeltus fasciatus: novel roles for hox genes in the hemipteran head. Development 127 (17), 3683–3694. https://doi.org/10.1242/dev.127.17.3683.

Hughes, C.L., Kaufman, T.C., 2002. Hox genes and the evolution of the arthropod body plan1. Evol. Dev. 4 (6), 459–499. https://doi.org/10.1046/j.1525-142X.2002.02034.x.

Khila, A., Abouheif, E., Rowe, L., 2009. Evolution of a novel appendage ground plan in water striders is driven by changes in the hox gene ultrabithorax. PLoS Genet. 5 (7), e1000583. https://doi.org/10.1371/journal.pgen.1000583.

Lawrence, J., Slipinski, A., 2013. Australian Beetles Volume 1: Morphology, Classification and Keys, vol. 1. CSIRO publishing.

Lemons, D., McGinnis, W., 2006. Genomic evolution of hox gene clusters. Science 313 (5795), 1918–1922. https://doi.org/10.1126/science.1132040.

Lewis, E.B., 1978. A gene complex controlling segmentation in drosophila. Nature 276 (5688), 565–570. https://doi.org/10.1038/276565a0.

Linz, D.M., Moczek, A.P., 2020. Integrating evolutionarily novel horns within the deeply conserved insect head. BMC Biol. 18 (1), 41. https://doi.org/10.1186/s12915-020-00773-9.

Linz, D.M., Hu, Y., Moczek, A.P., 2019. The origins of novelty from within the confines of homology: the developmental evolution of the digging tibia of dung beetles. ProcR Soc B Biol Sci 286, 20182427.

Madeira, F., Madhusoodanan, N., Lee, J., Eusebi, A., Niewielska, A., Tivey, A.R., Lopez, R., Butcher, S., 2024. The EMBL-EBI job dispatcher sequence analysis tools framework in 2024. Nucleic Acids Res. 52 (W1), W521–W525. https://doi.org/10.1093/nar/gkae241. PMID: 38597606.

Merrill, VKL, Diederich, RJ, Turner, FR, Kaufman, TC, 1989. A genetic and developmental analysis of mutations in *labial,* a gene necessary for proper head formation in *Drosophila melanogaster*. Developmental Biology 135 (2), 376–391.

Moczek, A.P., Nagy, L.M., 2005. Diverse developmental mechanisms contribute to different levels of diversity in horned beetles. Evol. Dev. 7 (3), 175–185. https://doi.org/10.1111/j.1525-142X.2005.05020.x.

Moczek, AP, Rose, DJ, 2009. Differential recruitment of limb patterning genes during development and diversification of beetle horns. PNAS 106 (22), 8992–8997.

Mulhair, P.O., Holland, P.W.H., 2022. Evolution of the insect hox gene cluster: comparative analysis across 243 species. Semin. Cell Dev. Biol. https://doi.org/10.1016/j.semcdb.2022.11.010.

Negre, B., Ruiz, A., 2007. HOM-C evolution in drosophila: is there a need for hox gene clustering? Trends Genet. 23 (2), 55–59. https://doi.org/10.1016/j.tig.2006.12.001.

Ohde, T., Yaginuma, T., Niimi, T., 2013. Insect morphological diversification through the modification of wing serial homologs. Science 340 (6131), 495–498. https://doi.org/10.1126/science.1234219.

Öztürk-Çolak, A, Marygold, SJ, Antonazzo, G, Attrill, H, Goutee-Gattat, D, Jenkins VK, & Tabone, CJ, 2024. FlyBase: updates to the *Drosophila* genes and genomes database. Genetics 227 (1), iyad211.

Pechmann, M, Schwager, EE, Turetzek, N, Prpic, N-M, 2015. Regressive evolution of the arthropod tritocerebral segment linked to functional divergence of the Hox gene *labial*. Proceedings of the Royal Society B: Biological Sciences 282 (1814), 20151162.

Philip, B.N., Tomoyasu, Y., 2011. Gene knockdown analysis by double-stranded RNA injection. In: Molecular Methods for Evolutionary Genetics, pp. 471–497.

Posnien, N., Bucher, G., 2010. Formation of the insect head involves lateral contribution of the intercalary segment, which depends on Tc-labial function. Dev. Biol. 338 (1), 107–116. https://doi.org/10.1016/j.ydbio.2009.11.010.

Posnien, N., Koniszewski, N.D.B., Hein, H.J., Bucher, G., 2011. Candidate gene screen in the red flour beetle tribolium reveals Six3 as ancient regulator of anterior median head and central complex development. PLoS Genet. 7 (12), e1002416. https://doi.org/10.1371/journal.pgen.1002416.

Posnien, N., Schinko, J.B., Kittelmann, S., Bucher, G., 2010. Genetics, development and composition of the insect head – a beetle's view. Arthropod Struct. Dev. 39 (6), 399–410. https://doi.org/10.1016/j.asd.2010.08.002.

Rogers, B.T., Kaufman, T.C., 1997. Structure of the insect head in ontogeny and phylogeny: a view from drosophila. In: Jeon, K.W. (Ed.), International Review of Cytology, vol 174. Academic Press, pp. 1–84. https://doi.org/10.1016/S0074-7696(08)62115-4.

Rogers, B.T., Peterson, M.D., Kaufman, T.C., 2002. The development and evolution of insect mouthparts as revealed by the expression patterns of gnathocephalic genes. Evol. Dev. 4 (2), 96–110. https://doi.org/10.1046/j.1525-142X.2002.01065.x.

Shafiei, M., Moczek, A.P., Nijhout, H.F., 2001. Food availability controls the onset of metamorphosis in the dung beetle Onthophagus taurus (coleoptera: scarabaeidae). Physiol. Entomol. 26 (2), 173–180. https://doi.org/10.1046/j.1365-3032.2001.00231.x.

Simonnet, F., Moczek, A.P., 2011. Conservation and diversification of gene function during mouthpart development in onthophagus beetles: gene function during mouthpart development in beetles. Evol. Dev. 13 (3), 280–289. https://doi.org/10.1111/j.1525-142X.2011.00479.x.

Smith, F.W., Jockusch, E.L., 2014. Hox genes require homothorax and extradenticle for body wall identity specification but not for appendage identity specification during metamorphosis of Tribolium castaneum. Dev. Biol. 395 (1), 182–197. https://doi.org/10.1016/j.ydbio.2014.08.017.

Smith, F.W., Boothby, T.C., Giovannini, I., Rebecchi, L., Jockusch, E.L., Goldstein, B., 2016. The compact body plan of tardigrades evolved by the loss of a large body region. Curr. Biol. 26 (2), 224–229. https://doi.org/10.1016/j.cub.2015.11.059.

Snodgrass, R.E., 1935. Principles of Insect Morphology. Cornell University Press.

Steinmann, H., Zombori, L., 2012. Dictionary of Insect Morphology, vol. 4. Walter de Gruyter.

Tschopp, P., Duboule, D., 2011. A regulatory 'landscape effect' over the HoxD cluster. Dev. Biol. 351 (2), 288–296. https://doi.org/10.1016/j.ydbio.2010.12.034.

Tschopp, P., Fraudeau, N., Béna, F., Duboule, D., 2011. Reshuffling genomic landscapes to study the regulatory evolution of hox gene clusters. Proc. Natl. Acad. Sci. 108 (26), 10632–10637. https://doi.org/10.1073/pnas.1102985108.

Wang, Y., Tang, H., Wang, X., et al., 2024. Detection of colinear blocks and synteny and evolutionary analyses based on utilization of MCScanX. Nat. Protoc. 19, 2206–2229. https://doi.org/10.1038/s41596-024-00968-2.

Yao, L.-C., Liaw, G.-J., Pai, C.-Y., Sun, Y.H., 1999. A common mechanism for antenna-to-leg transformation in drosophila: suppression of homothorax transcription by four HOM-C genes. Dev. Biol. 211 (2), 268–276. https://doi.org/10.1006/dbio.1999.9309.

Zattara, E.E., Busey, H.A., Linz, D.M., Tomoyasu, Y., Moczek, A.P., 2016. Neofunctionalization of embryonic head patterning genes facilitates the positioning of novel traits on the dorsal head of adult beetles. Proc. Biol. Sci. 283 (1834), 20160824. https://doi.org/10.1098/rspb.2016.0824.

Zhang, R., Zhang, Z., Yu, Y., Huang, Y., Qian, A., Tan, A., 2020. Proboscipedia and sex combs reduced are essential for embryonic labial palpus specification in Bombyx mori. J. Integr. Agric. 19 (6), 1482–1491. https://doi.org/10.1016/S2095-3119(19)62785-1.

Schaeper ND, Pechmann M, Damen WGM, Prpic N-M. Wimmer EA. 2010. Evolutionary plasticity of collier function in head development of diverse arthropods. Developmental Biology. 344(1):363-376.